Journal of Ceramic Processing Research. Vol. 21, No. 1, pp. 92~98 (2020)
(Received 4 October 2019, Received in revised form 24 December 2019, Accepted 26 December 2019)
https://doi.org/10.36410/jcpr.2020.21.1.92

J O U R N A L O F
Ceramic Processing Research

Thermal shock resistance of TaC/SiC coatings on carbon/carbon composites by the CVD process

Hyun-Mi Kim[a,b], Sung-Churl Choi[b], Yeontae Kim[c], Hyung Ik Lee[c] and Kyoon Choi[a,*]
[a]*Engineering Ceramic Center, KICET, Icheon, 17303, Korea*
[b]*Division of advanced Materials Science and Engineering, Hanyang Univ., Seoul, 04763, Korea*
[c]*The 4th R&D Institute, Agency for Defense Development, Daejon, 34186, Korea*

Carbon/carbon composites (C / C) have been widely studied in the aerospace field given their excellent thermal shock resistance and specific strength at high temperatures. However, they are associated with the problem of rapid oxidization and deterioration under normal atmospheric environments. In order to overcome these problems, chemical vapor deposition (CVD) coatings of ultra-high temperature ceramics to C / C have become an important technical step. In this study, TaC coatings on C / C were carried out by a CFD simulation and a subsequent CVD process. A TaC monolayer and a SiC / TaC / SiC / TaC multilayer were compared with respect to the degree of thermal shock resistance, accomplished in this case with an arc heater. The TaC monolayer was mostly delaminated on the horizontally oriented carbon fibers, which resulted in sharpened carbon fibers and porous Ta_2O_5 layers. However, the multilayer structure showed a protective vitreous coating due to the oxidation of the SiC layer, with the inner C / C successfully protected by the porous Ta_2O_5 layer underneath. It can be concluded that multilayer coatings of SiC / TaC / SiC / TaC can be more effective for thermal shock and oxidation resistance capabilities of composites.

***Keywords*: Ultra high temperature ceramics, Chemical vapor deposition, Tantalum carbide, Thermal shock resistance**

Introduction

The C / C composite is a high-temperature structural material with a low density level, a small coefficient of thermal expansion, and high specific strength, making it an ideal material as a thermal barrier of aircraft nose tips, leading edges and reentry vehicles. In most cases, however, these applications require oxidation and ablation resistance and therefore require an appropriate coating layer for the protection of the C / C [1]. UHTC carbides such as TaC, HfC, and ZrC can be used in an oxidizing atmosphere because they have not only high melting points of the carbides but also high melting points after the oxidation of the carbides [2, 3]. After oxidation, however, a porous layer is formed such that the inflow of oxygen into the interior is inevitable. Accordingly, gastight characteristics can be expected via the formation of a multilayer as opposed to using this approach alone [4].

As a multilayer material that complements the oxidation resistance of UHTC carbide, silicon-based phases such as SiC and $MoSi_2$ can help maintain a suitable level of oxidation resistance [5, 6]. The multilayer forms an SiO_2-based amorphous layer that can prevent permeation of a gas even when oxidized, thereby allowing the internal C / C to be preserved at temperatures below 1400 degrees Celsius [2]. As a means of forming the UHTC carbide and silicon carbide multilayer, CVD [7], SAPS (supersonic atmosphere plasma spraying) [8, 9], pack cementation [10], and slurry coating [11], have been used. The simplest and most stable method is to form a multi-coating layer by CVD.

In this study, the heat-resistant oxidation characteristics of two coating layers of TaC and SiC / TaC / SiC / TaC were compared based on TaC and SiC as protective coatings for the oxidation and ablation of C / C. In addition, a computational fluid dynamics simulation was used to improve the uniformity of the coating layer.

Experimental

The raw materials and equipment used for the experiments were detailed in a previously published paper [12, 13]. TaCl5 (99.5%, H.C. Starck, Germany), used as a raw material, was put into a vaporizer using a powder feeder capable of delivering the powder at a constant rate in the form of a solid powder. As a carrier gas, hydrogen gas containing 5% CH_4 was used, with the gas mixed with $TaCl_5$ in the vaporizer at 230 degrees Celsius and delivered along a heated gas line to the inlet, as shown in Fig. 1.

*Corresponding author:
Tel : +82-31-645-1456
Fax: +82-31-645-1493
E-mail: knchoi@kicet.re.kr

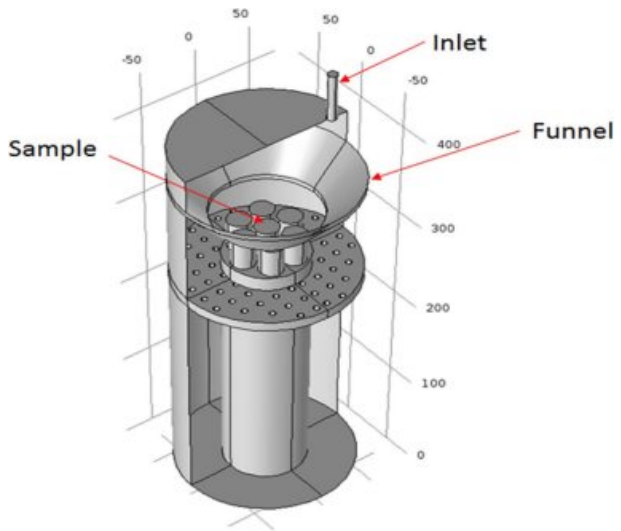

Fig. 1. Schematics of the sample location in the deposition chamber for the TaC and SiC coating.

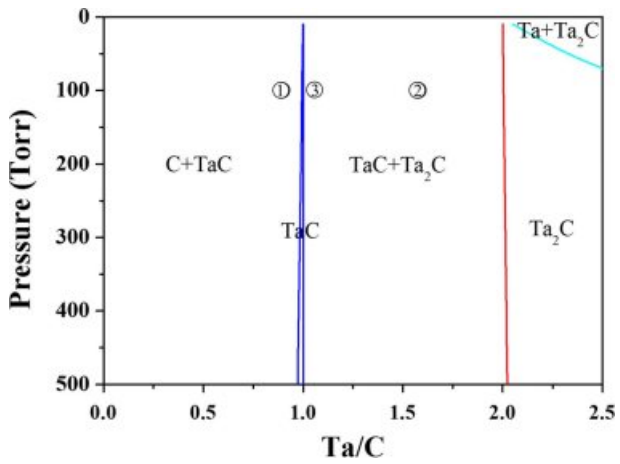

Fig. 2. Thermodynamic phase diagram at 1200 °C with CH_4 5% hydrogen and $TaCl_5$ as the gas sources

The C / C sample was provided by DACC Co., Ltd. It was cylindrical with a diameter of 15 mm and height of 50 mm. First, all samples were coated with silicon carbide to a depth of 35 μm, after which 50 μm of TaC or 50 μm of SiC / TaC / SiC / TaC were alternately raised and the microstructures and heat resistance characteristics compared. The deposition conditions for the silicon carbide and TaC are summarized in Table 1.

As shown in Table 1, hydrogen gas bubbling through a bubbler containing an MTS liquid was transported to the reactor for the silicon carbide, while the mixed hydrogen gas containing $TaCl_5$ vapor controlled by the powder feeder was provided for the tantalum carbide. Therefore, the SiC / TaC multi-coating structure can be formed using deposition processes alternately through two lines. The C / C composite sample produced through this process was subjected to a thermal shock test using a 200 kW arc heater. After the surface was subjected to a phase analysis by XRD, the components remaining on the surface were confirmed by FE-SEM and EDS.

Results and Discussion

Phase prediction with FactSage 6.2

Fig. 2 shows the phase equilibrium when 5% CH_4 containing hydrogen and $TaCl_5$ are used as the raw materials. In this system, a mixed phase of C and TaC or a mixed phase of TaC and Ta_2C is more easily obtained than a single TaC phase because the TaC single-phase region is obtained only in a narrow region where the ratio of Ta and C is one. Therefore, two microstructures were compared to determine the condition under which the heat resistance characteristics are expected to be better.

The microstructure obtained under the condition 1 shown in Fig. 2 demonstrated a mixed phase of C and TaC, where small TaC crystals were distributed in the pyrolytic carbon matrix, as shown in Fig. 3(a). This can also be observed in the SAED pattern in Fig. 3(b) and in the HRTEM image in Fig. 3(c), in which several nanometer-sized TaC crystals can be distinguished. The microstructure is expected to be inadequate as an anti-ablation coating due to the pyrolytic carbon constituting the matrix. On the other hand, the microstructure obtained under condition 2 in Fig. 2 presents a mixed phase of TaC and Ta_2C, in which case micrometer-sized TaC and Ta_2C crystals are homogeneously mixed. If TaC and Ta_2C crystals are mixed, each will likely prevent the growth of the other to therefore maximize the heat resistance and anti-ablation characteristics. Other studies [13-16] have reported that the heat-resistance and anti-ablation properties of these types of coatings deteriorate when TaC crystals grow in the form of a columnar structure. Therefore, the sample was prepared under condition 3 in Fig. 2 because this condition utilized the maximum amount of TaC for excellent ablation resistance while at the same time suppressing the coarsening of the TaC crystals due to the small amount of Ta_2C.

CFD prediction for a uniform deposition

The sample holder was fabricated to deposit seven cylindrical heat-resistant samples at the same time, and a funnel was installed on top of it. The purpose of this

Table 1. Details of experimental conditions for SiC and TaC deposition processes.

Materials deposited	Pressure	Temperature	Source materials and evaporation tools	Carrier gas	Gas flow rate
SiC	10 Torr	1200 °C	Methyltrichlorosilane (MTS: CH_3SiCl_3) and bubbler	hydrogen	5 slm
TaC	100 Torr	1200 °C	$TaCl_5$ and powder feeder	5% CH_4 + 95% H_2	1.5 slm

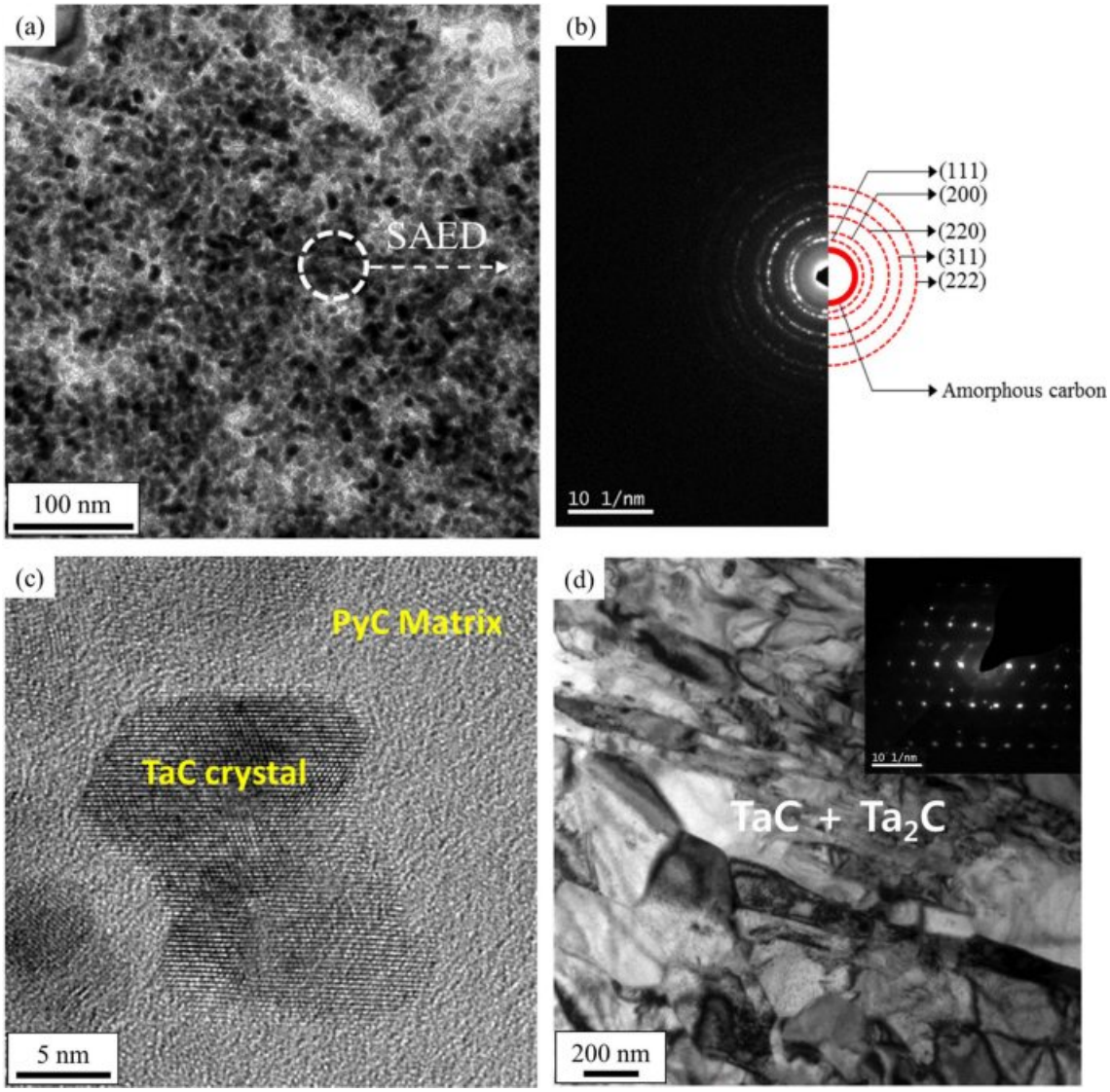

Fig. 3. TEM micrographs of (a) a specimen deposited under condition "1," (b) corresponding SAED pattern, (c) high-resolution image, and (d) a sample deposited under condition "2" in Fig. 2.

installation was to reduce the thickness deviation between the samples. The change of the flow rate distribution before and after the installation of the funnel was confirmed through a CFD analysis, the results of which are shown in Fig. 4. Checking the velocity contours at positions "A" and "B" in Fig. 4(a), a steep slope of the velocity is found at "B." In contrast, the velocity distribution is much more uniform in the "C" and "D" positions after the installation of the funnel, as shown in Fig. 4(b). The reactant gas is well guided over the specimen by the funnel to increase the deposition rate, as shown in Fig. 4(d).

TaC was deposited at positions "A" and "B" to demonstrate experimentally the large difference in the flow velocity distributions in Fig. 4(a). A film of TaC with a small amount of Ta_2C was formed after four hours of deposition under condition 3 in Fig. 2. Significant differences in the thickness at the "B" site were found at the right and left ends of the sample, as shown in Figs. 5(a) and 5(b), respectively. On the other hand, at the "A" site, a very thin TaC layer was identified, as shown in Fig. 5(c).

Deposition of the TaC/SiC multilayer

The cross-sectional microstructures of the TaC layer and the SiC / TaC / SiC / TaC multilayer are shown in Figs. 6, and these are used in the high heat flow experiments. It can be seen that a coating layer of approximately 80 to 100 μm is added onto the 35 μm SiC intermediate layer on the C / C. Silicon carbide layers occasionally have irregular or porous surfaces that appear to have complex interfaces with TaC.

High heat flux experiment on the TaC monolayer deposited C / C

The sample of the TaC monolayer showed a severe

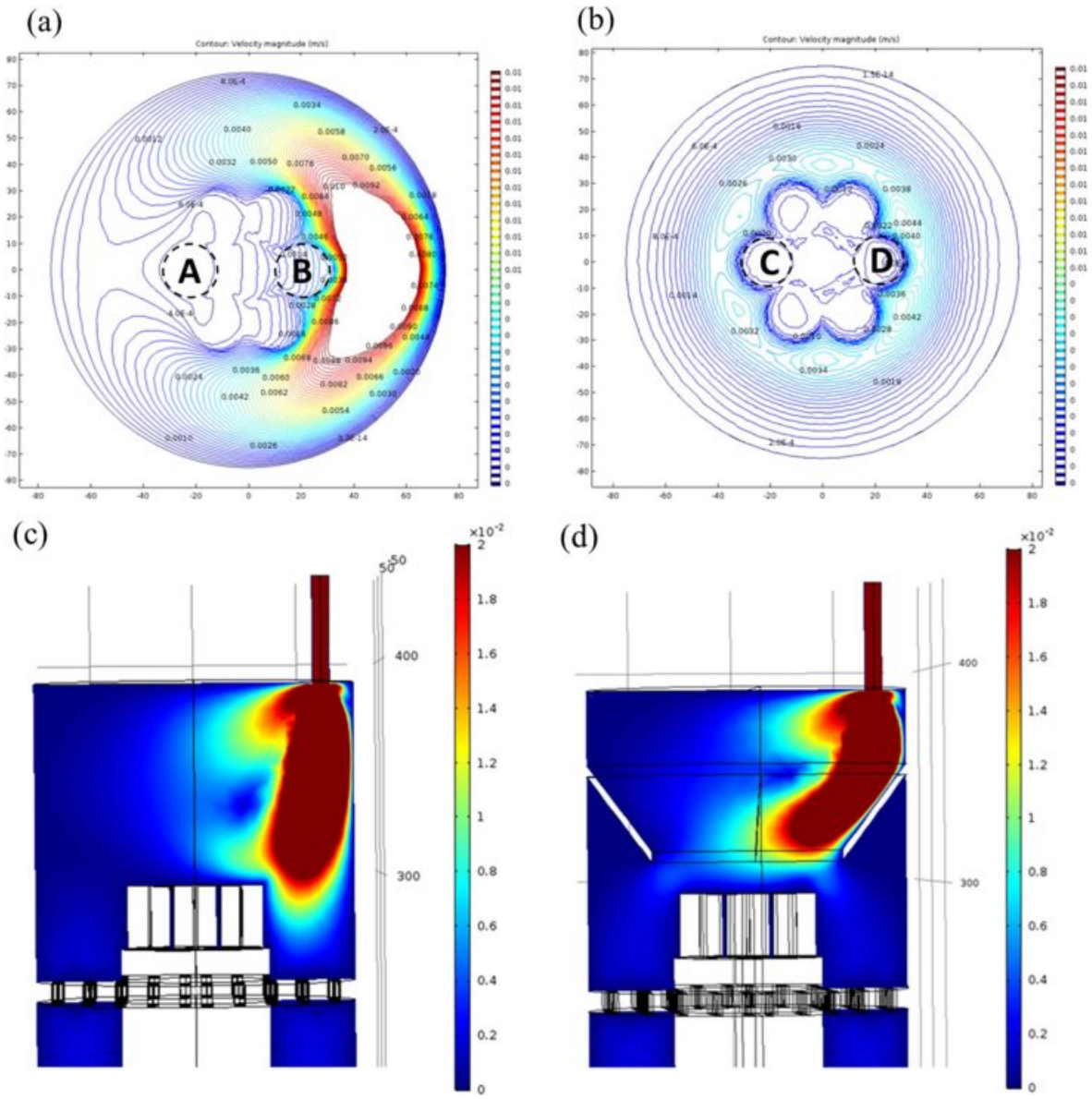

Fig. 4. Comparison of the surface velocity (a) without and (b) with the funnel designed to reduce the uniformity of the film thickness, and cross-sectional profile of the velocity distribution (c) without and (d) with the funnel.

appearance change after the heat flux experiment. A large part of the coating layer had peeled off, and the outer surface of the sample appeared to form a porous coating layer composed of the Ta_2O_5 crystal phase. This is clearly observable in Fig. 7 in the XRD results, which shows strong carbon peaks indicating the significant portion of C / C exposure, with only the Ta_2O_5 crystal phase and underlying SiC layer identifiable. A long strap peeled off due to the large difference in the thermal expansion coefficient between the coating layer and the C / C, as shown in Fig. 8. Most of the C / C exposed areas are those in which the carbon fibers are horizontally oriented. It was also confirmed that the tip of the carbon fiber is sharply oxidized, as shown in Fig. 9(b). The carbon fibers are thought to have been exposed at the beginning of the high heat flux experiment. According to the weaving direction of the carbon fiber, it could be confirmed as to whether the Ta_2O_5 layer is attached. It was noted that Ta_2O_5, which appears as a bright area, scarcely remains in the area where it horizontally comes into contact with the carbon fiber.

High heat flux experiment on multilayer deposited C / C

Fig. 10 shows the appearance after the high heat flux test of the samples with the SiC / TaC / SiC / TaC multilayers to a thickness of 50 μm. It was confirmed that a white oxide layer had formed along the outer edge of the sample, with partial peeling also observed. The XRD results show that part of the TaC layer was oxidized to Ta_2O_5 but that some TaC remains robust

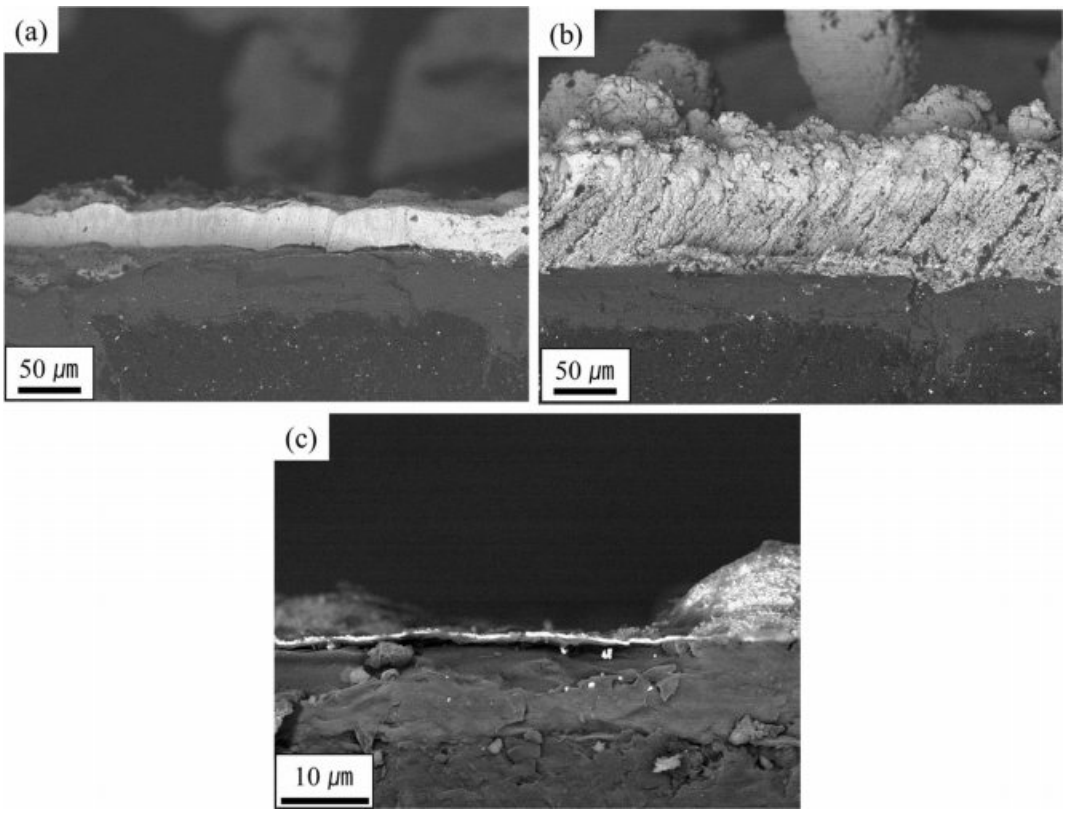

Fig. 5. Cross-sectional micrographs of (a) the left side and (b) right side of specimen "B" and (c) specimen "A" designated in Fig. 4(a).

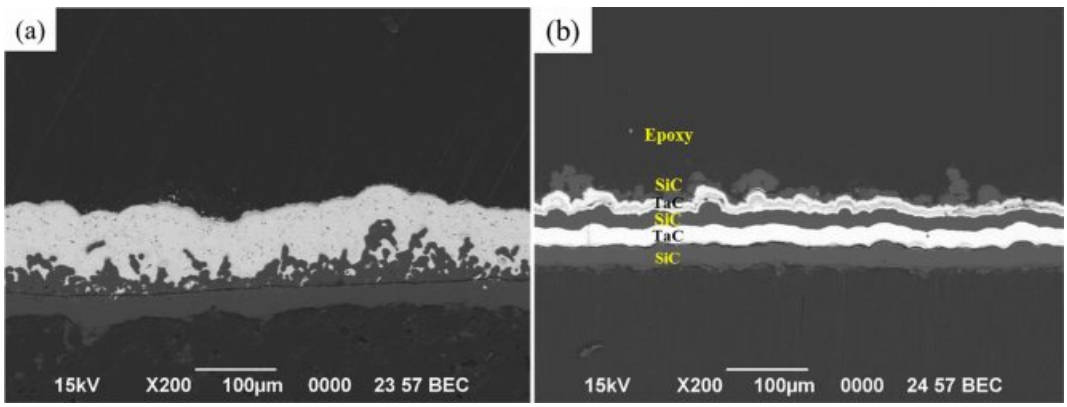

Fig. 6. Cross-sectional SEM micrographs of the (a) TaC layer and (b) SiC / TaC / SiC / TaC multilayer.

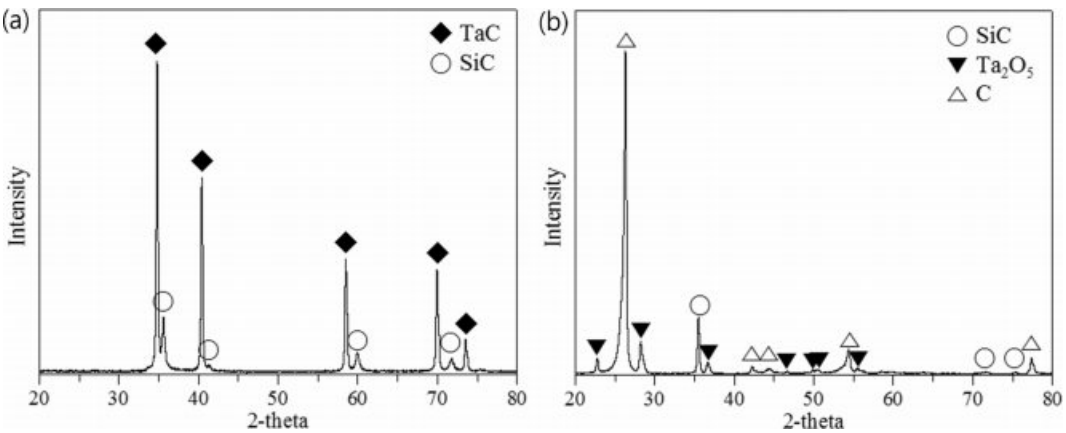

Fig. 7. XRD results of the TaC layer (a) before and (b) after the high heat flux experiment.

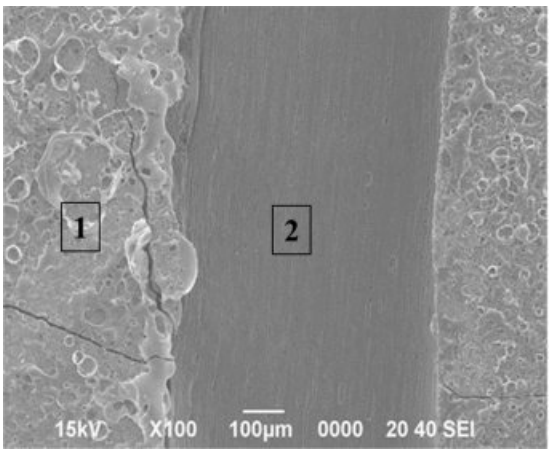

Fig. 8. SEM micrographs of the TaC layer showing local peel off regions after the high heat flux experiment.

under the SiC layer. The silicon carbide layer on the surface was vitrified as it was oxidized, as shown in Fig. 11(b). With the flow of the high heat flux, liquid silicate formed, appearing to flow downward. Meanwhile, the TaC layer underneath is partially oxidized to form a Ta_2O_5 layer. As shown in Fig. 11(c), it has a porous appearance, similar to the microstructures observed in other studies [17, 18]. It is estimated that the melting and covering of the silicate glass on TaC protects against further oxidation of the TaC layers, while the C / C can also be protected from oxidation.

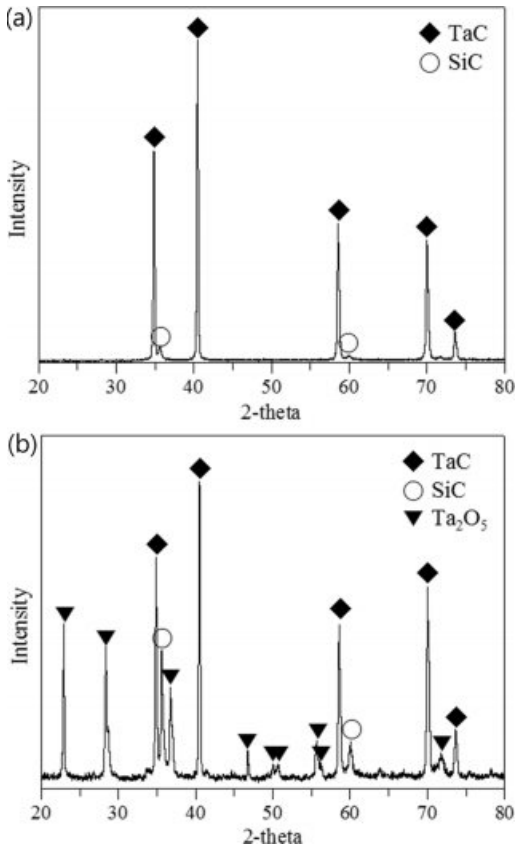

Fig. 10. XRD results of the SiC / TaC / SiC / TaC multilayer (a) before and (b) after the high heat flux experiment.

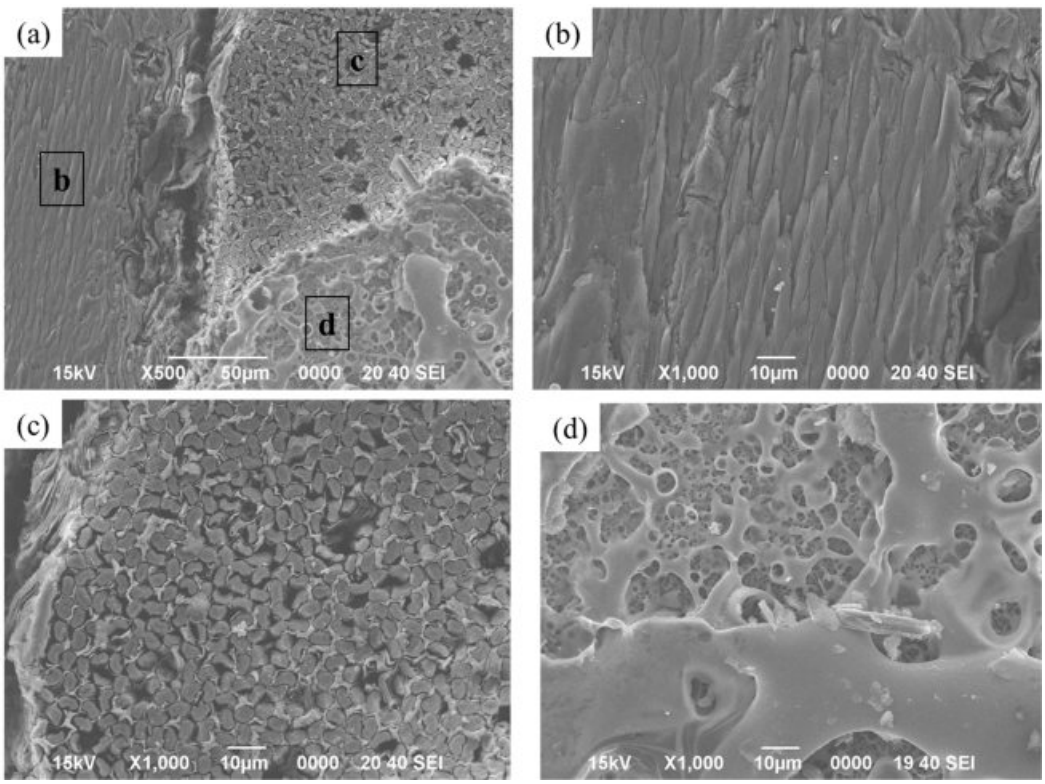

Fig. 9. SEM micrographs of the TaC layer after the high heat flux experiment: (a) surface and (b), (c), and (d) marked local magnifications of (a).

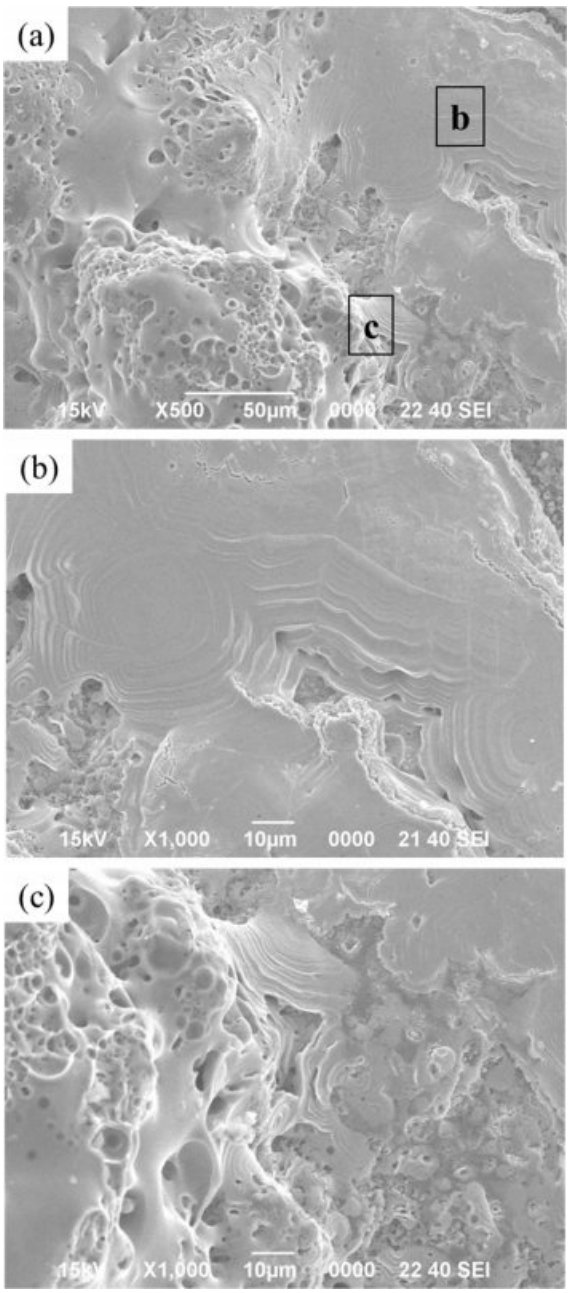

Fig. 11. SEM micrographs of the SiC / TaC / SiC / TaC multilayers after the high heat flux experiment: (a) surface and (b), (c) denoted local magnifications of (a).

Conclusion

The combination of the oxidation resistance of SiC and the abrasion resistance of TaC to form a new combination of UHTC coating layers has been tried. TaC monolayers with a TaC phase containing trace amounts of the Ta_2C phase were CVD-coated on SiC-coated C / C and high thermal flux experiments were carried out. After the high heat flux experiments, exfoliation of the TaC layers occurred depending on the fiber arrangement of the C / C, with severe morphological changes. One the other hand, the SiC / TaC / SiC / TaC multilayers on SiC-coated C / C showed no delamination. For the multilayer-coated samples, the internal TaC film mostly survived after the high thermal flux experiments, most likely due to silicate formation caused by the oxidation of the SiC top layer. Microstructures on which the liquid silicate flowed down to a porous Ta_2O_5 layer were frequently observed.

Acknowledgement

This work was supported by the Korean Government (Defense Acquisition Program Administration, DAPA) through research institute (Agency for Defense Development, ADD).

References

1. M.E. Westwood, J.D. Webster, R.J. Day, F.H. Hayes, and R. Taylor, J. Mater. Sci. 31[6] (1996) 1389-1397.
2. M.M. Opeka, I.G. Talmy, and J.A. Zaykoski, J. Mater. Sci. 39[19] (2004) 5887-5904.
3. E.L. Corral and R.E. Loehman, J. Am. Ceram. Soc. 91[5] (2008) 1495-1502.
4. F. Lamouroux, S. Bertrand, R. Pailler, and R. Naslain, Key Eng. Mater. 164 (1998) 365-368.
5. Q. Fu, X. Zou, Y. Chu, H. Li, J. Zou, and C. Gu, Vacuum 86[12] (2012) 1960-1963.
6. Y.-L. Zhang, H.-J. Li, X.-F. Qiang, K.-Z. Li, and S.-Y. Zhang, Corros. Sci. 53[11] (2011) 3840-3844.
7. G.-d. Li, X. Xiong, B.-y. Huang, and K.-l. Huang, Trans. Nonferrous Met. Soc. 18[2] (2008) 255-261.
8. Y. Zhang, H. Hu, P. Zhang, Z. Hu, H. Li, and L. Zhang, Surf. Coat. Tech. 300[25](2016)1-9.
9. Y. Zhang, Z. Hu, H. Li, and J. Ren, Ceram.Int. 40[9] (2014)14749-14755.
10. P. Wang, S. Zhou, P. Hu, G. Chen, X. Zhang, and W. Han, J. Alloy Compd. 682[15] (2016) 203-207.
11. S. Ramasamy, S.N. Tewari, and K.N. Lee, Mater. Sci. Eng. A 527[21-22] (2010) 5492–5498.
12. H.-M. Kim, K. B. Shim, J.-M. Lee, H.-I Lee, and K. Choi, J. Ceram. Proc. Res. 19[6] (2018) 519-524.
13. Y.-S. Jeong, K. Choi, and H.G. Yoon, J. Korean Ceram. Soc. 56[3] (2019) 291-297.
14. Y. Wang, X. Xiong, G. Li, Z. Chen, W. Sun, and X. Zhao, Corros. Sci. 65 (2012) 549-555.
15. Y. Wang, X. Xiong, G. Li, X. Zhao, Z. Chen, W. Sun, and Z. Wang, Solid State Sci. 20 (2013) 86-91.
16. Y. Wang, Z. Li, X. Xiong, X. Li, Z. Chen, and W. Sun, Appl. Surf. Sci. 390 (2016) 903-908.
17. C. Zhen, X. Xiong, G. Li, W. Sun, and Y. Long, Appl. Surf. Sci. 257 (2010) 656-661.
18. G. Li, X. Xiong, and K. Huang, Trans. Nonferrous Met. Soc. 18 (2008) s689-s695.